Optimal knots selection in fitting degenerate reduced data

Ryszard Kozera[1,2][0000−0002−2907−8632] and Lyle Noakes[2][0000−0001−9595−0735]

[1] Institute of Information Technology, Warsaw University of Life Sciences - SGGW, ul. Nowoursynowska 159, 02-776 Warsaw, Poland
ryszard_kozera@sggw.edu.pl
ryszard.kozera@gmail.com
[2] School of Physics, Mathematics and Computing, The University of Western Australia, 35 Stirling Highway, Crawley, WA 6009, Perth, Australia
{ryszard.kozera,lyle.noakes}@uwa.edu.au

Abstract. The problem of fitting a given ordered sample of data points in arbitrary Euclidean space is addressed. The corresponding interpolation knots remain unknown and as such must be first somehow found. The latter leads to a highly non-linear multivariate optimization task, equally non-trivial for theoretical analysis and for derivation of a computationally efficient numerical scheme. The non-degenerate case of at least four data points can be handled by Leap-Frog algorithm merging generic and non-generic univariate overlapping optimizations. Sufficient conditions guaranteeing the unimodality for both cases of Leap-Frog optimization tasks are already established in the previous research. This work complements the latter by analyzing the degenerate situation i.e. the case of fitting three data points, for which Leap-Frog cannot be used. It is proved here that the related univariate cost function is always unimodal yielding a global minimum assigned to the missing internal-point knot (with no loss both terminal knots can be assumed to be fixed). Illustrative examples supplement the analysis in question.

Keywords: Optimization · Curve Modelling · Data Fitting

1 Introduction

The problem of fitting data is a classical problem for which numerous interpolation techniques can be applied (see e.g. [1, 11, 16]). In classical setting, most of such schemes admit a sequence of $n+1$ input points $\mathcal{M}_n = \{x_n\}_{i=0}^n$ in arbitrary Euclidean space $\mathbb{E}^m$ accompanied by the sequence of the corresponding interpolation knots $\mathcal{T} = \{t_i\}_{i=0}^n$. The problem of data fitting and modeling gets complicated for the so-called *reduced data* for which only the points $\mathcal{M}_n$ are given. Here, for a given fitting scheme, different choices of ordered interpolation knots $\{\hat{t}_i\}_{i=0}^n$ render different curves. An early work on this topic can be found in [12] subsequently investigated e.g. in [10, 11]. In particular, various quantitative criteria (often for special $m = 2, 3$) are introduced to measure the

ICCS Camera Ready Version 2023
To cite this paper please use the final published version:
DOI: 10.1007/978-3-031-36024-4_34

suitability of a special choice of $\{\hat{t}_i\}_{i=0}^n$ - e.g. the convergence rate of the interpolant to the unknown curve once $\mathcal{M}_n$ is getting denser. A more recent work in which different parameterization of the unknown knots are discussed (including the so-called cumulative chord or its extension called the exponential parameterization) can be found e.g. in [2, 8, 11]. One of the approaches (see [3]) to substitute the unknown knots $\mathcal{T}_{n-1} = (t_1, t_2, \ldots, t_{n-1})$ (here one can set $t_0 = 0$ and $t_n = T$, e.g. with T as cumulative chord) is to minimize $\int_{t_0}^{t_n} \|\ddot{\gamma}^{NS}(t)\| dt$ subject to $0 < t_1 < t_2 < \ldots < t_{n-1} < T$, where $\gamma^{NS} : [0, T] \to \mathbb{E}^m$ defines a natural spline (see [1]) based on $\mathcal{M}_n$ and $\mathcal{T}_{n-1}$. Such constrained optimization task can be transformed into minimizing (see e.g. [3]) the following multivariate cost function:

$$\mathcal{J}(t_1, t_2, \ldots, t_{n-1}) = 4 \sum_{i=0}^{n-1} \Big(\frac{-1}{(\Delta t_i)^3} (-3\|x_{i+1} - x_i\|^2 + 3\langle v_i + v_{i+1} | x_{i+1} - x_i \rangle \Delta t_i - (\|v_i\|^2 + \|v_{i+1}\|^2 + \langle v_i | v_{i+1} \rangle)(\Delta t_i)^2 \Big) , \quad (1)$$

where the set $\{v_i\}_{i=0}^n$ represents the respective velocities at $\mathcal{M}_n$ which are expressible in terms of $\mathcal{M}_n$ and parameters $\mathcal{T}_{n-1}$ (see [1]). The latter constitutes a highly non-linear multivariate optimization task difficult to analyze and to solve numerically (see [4]). For technical reason it is also assumed that $x_i \neq x_{i+1}$, for $i = 1, 2, \ldots, n-1$. Leap-Frog algorithm is a possible remedy here ($n \geq 3$ yields a non-degenerate case of (1) yielding at least four interpolation points) which with the aid of iterative overlapping univariate optimizations (generic and non-generic one) computes a critical point $(t_1^{opt}, t_2^{opt}, \ldots, t_{n-1}^{opt})$ to (1). More information on Leap-Frog in the context of minimizing (1) together with the analysis on establishing sufficient conditions enforcing the unimodality of the respective univariate cost functions can be found in [6, 7].

This work[3] extends theoretical analysis on minimizing (1) via Leap-Frog algorithm (performed for $n \geq 3$) to the remaining degenerate case of $n = 2$. Here neither generic nor non-generic case of Leap-Frog is applicable. Indeed for the univariate generic Leap-Frog optimization (see [6]) both velocities in the k-iteration process i.e. v_i^k and v_{i+2}^k (at points x_i and x_{i+2}, respectively) are assumed to be temporarily fixed and a local complete spline $\gamma_i^C : [t_i^k, t_{i+2}^k] \to \mathbb{E}^m$ (see [1]) is used to recompute the knot t_{i+1}^{k-1} to t_{i+1}^k and consequently the velocity v_{i+1}^{k-1} to v_{i+1}^k (at point x_{i+1}) upon minimizing $\mathcal{E}_i(t_{i+1}) = \int_{t_i^k}^{t_{i+2}^k} \|\ddot{\gamma}_i^C(t)\| dt$. Similarly univariate non-generic Leap-Frog optimization (see [7]) relies on $a_0 = \mathbf{0}$ and v_2^k or on v_{n-2}^k and $a_n = \mathbf{0}$ given (with velocities v_2^k and v_{n-2}^k fed by generic Leap-Frog iterations), where a_0 and a_n represent the corresponding accelerations fixed at x_0 and x_n, respectively. Here knots t_1^{k-1} (and t_{n-1}^{k-1}) are recomputed into t_1^k (and t_{n-1}^k) with the corresponding velocities v_1^{k-1} (and v_{n-1}^{k-1}) updated to v_1^k (and v_{n-1}^k). For the exact local energy formulation and the related analysis see [7].

[3] This work is a part of Polish National Centre of Research and Development Project POIR.01.02.00-00-0160/20.

Noticeably for $n = 2$ (i.e. degenerate case of reduced data with three interpolation points) accompanied by $a_0 = \mathbf{0}$ and $a_2 = \mathbf{0}$ minimizing (1) reformulates into:

$$\mathcal{E}_{deg}(t_1) = \mathcal{J}(t_1) = 4\sum_{i=0}^{1}\Big(\frac{-1}{(\Delta t_i)^3}(-3\|x_{i+1}-x_i\|^2 + 3\langle v_i + v_{i+1}|x_{i+1}-x_i\rangle\Delta t_i - (\|v_i\|^2 + \|v_{i+1}\|^2 + \langle v_i|v_{i+1}\rangle)(\Delta t_i)^2\Big) , \quad (2)$$

which does not fall into one of the Leap-Frog so-far derived schemes (i.e. generic and non-generic case handling $\mathcal{M}_n$ with $n \geq 3$).

In this paper we prove the unimodality of (2) and supplement illustrative examples. Consequently, computing the optimal knot t_1 is not susceptible to the initial guess and forms a global minimum of (2). Fitting reduced data $\mathcal{M}_n$ via optimization (1) (or with other schemes replacing the unknown knots $\mathcal{T}$) applies in modeling [16] (e.g. computer graphics and computer vision), in approximation and interpolation [5, 11] (e.g. trajectory planning, length estimation, image segmentation or data compression) as well as in many other engineering and physics problems [13] (e.g. robotics or particle trajectory estimation).

2 Degenerate Case: First and Last Accelerations Given

Assume that for three data points $x_0, x_1, x_2 \in \mathcal{M}_n$ (for $n = 2$) the interpolation knots t_0 and t_2 are somehow known together with respective first and terminal accelerations $a_0, a_2 \in \mathbb{R}^m$. In fact, one can safely assume here (upon coordinate shift and rescaling) that $t_0 = 0$ and $t_2 = T_{cc} = \|x_1 - x_0\| + \|x_2 - x_1\|$ representing a cumulative chord parameterization. Let a C^2 piecewise cubic (depending on varying $t_1 \in (t_0, t_2)$) denoted by $\gamma^c_{deg} : [t_0, t_2] \to \mathbb{E}^m$ (i.e. a cubic on each $[t_0, t_1]$ and $[t_1, t_2]$) satisfy:

$$\gamma^c_{deg}(t_j) = x_j \ , \quad j = 0, 1, 2 \ ; \qquad \ddot{\gamma}^c_{deg}(t_j) = a_k \ , \quad k = 0, 2 \ ,$$

and be C^2 class over $[t_0, t_2]$. Upon introducing the mapping $\phi_{deg} : [t_0, t_2] \to [0, 1]$

$$\phi_{deg}(t) = \frac{t - t_0}{t_2 - t_0} \quad (3)$$

the reparameterized curve $\tilde{\gamma}^c_{deg} : [0, 1] \to \mathbb{E}^m$ defined as $\tilde{\gamma}^c_{deg} = \gamma^c_{deg} \circ \phi^{-1}_{deg}$ satisfies, for $0 < s_1 < 1$ (where $s_1 = \phi_{deg}(t_1)$):

$$\tilde{\gamma}^c_{deg}(0) = x_0 \ , \quad \tilde{\gamma}^c_{deg}(s_1) = x_1 \ , \quad \tilde{\gamma}^c_{deg}(1) = x_2 \ ,$$

with the adjusted first and terminal accelerations $\tilde{a}_0, \tilde{a}_2 \in \mathbb{R}^m$

$$\tilde{a}_0 = \tilde{\gamma}^{c''}_{deg}(0) = (t_2 - t_0)^2 a_0 \ , \quad \tilde{a}_2 = \tilde{\gamma}^{c''}_{deg}(1) = (t_2 - t_0)^2 a_2 \ . \quad (4)$$

ICCS Camera Ready Version 2023
To cite this paper please use the final published version:
DOI: 10.1007/978-3-031-36024-4_34

Remark 1. An easy inspection shows (for each $s_1 = \phi_{deg}(t_1)$) that $\tilde{\mathcal{E}}_{deg}(s_1)$

$$= \int_0^1 \|\tilde{\gamma}_{deg}^{c''}(s)\| ds = (t_2 - t_0)^3 \int_{t_0}^{t_2} \|\ddot{\gamma}_{deg}^{c}(t)\|^2 dt = (t_2 - t_0)^3 \mathcal{E}_{deg}(t_1) \ . \quad (5)$$

Hence all critical points s_1^{crit} of $\tilde{\mathcal{E}}_{deg}$ are mapped (one-to-one) onto critical points $t_1^{crit} = \phi_{deg}^{-1}(s_1^{crit}) = s_1^{crit}(t_2 - t_0) + t_0$ of $\mathcal{E}_{deg}$. Consequently all optimal points of $\mathcal{E}_{deg}$ and $\tilde{\mathcal{E}}_{deg}$ are conjugated with $t_1^{opt} = \phi_{deg}^{-1}(s_1^{opt})$. □

We determine now the explicit formula for $\tilde{\mathcal{E}}_{deg}$. In doing so, for $\tilde{\gamma}_{deg}^{c}$ (with $s_1 \in (0,1)$ as additional parameter) define now (here $\tilde{\gamma}_{deg}^{lc}(s_1) = \tilde{\gamma}_{deg}^{lc}(s_1)$):

$$\tilde{\gamma}_{deg}^{c}(s) \ = \ \begin{cases} \tilde{\gamma}_{deg}^{lc}(s) \ , & \text{for } s \in [0, s_1] \\ \tilde{\gamma}_{deg}^{rc}(s) \ , & \text{for } s \in [s_1, 1] \end{cases}$$

where, with $c_j^{deg}, d_j^{deg} \in \mathbb{R}^m$ (for $j = 0,1,2,3$)

$$\tilde{\gamma}_{deg}^{lc}(s) = c_0^{deg} + c_1^{deg}(s - s_1) + c_2^{deg}(s - s_1)^2 + c_3^{deg}(s - s_1)^3 \ ,$$
$$\tilde{\gamma}_{deg}^{rc}(s) = d_0^{deg} + d_1^{deg}(s - s_1) + d_2^{deg}(s - s_1)^2 + d_3^{deg}(s - s_1)^3 \ ,$$

the following must hold:

$$\tilde{\gamma}_{deg}^{lc}(0) = x_0 \ , \quad \tilde{\gamma}_{deg}^{lc}(s_1) = \tilde{\gamma}_{deg}^{rc}(s_1) = x_1 \ , \quad \tilde{\gamma}_{deg}^{rc}(1) = x_2 \ , \quad (6)$$

and also

$$\tilde{\gamma}_{deg}^{lc''}(0) = \tilde{a}_0 \ , \qquad \tilde{\gamma}_{deg}^{rc''}(1) = \tilde{a}_2 \ , \quad (7)$$

together with the C^1 and C^2 class constraints at $s = s_1$:

$$\tilde{\gamma}_{deg}^{lc'}(s_1) = \tilde{\gamma}_{deg}^{rc'}(s_1) \ , \qquad \tilde{\gamma}_{deg}^{lc''}(s_1) = \tilde{\gamma}_{deg}^{rc''}(s_1) \ . \quad (8)$$

Without loss, we may assume that

$$\tilde{x}_0 = x_0 - x_1 \ , \quad \tilde{x}_1 = \mathbf{0} \ , \quad \tilde{x}_2 = x_2 - x_1 \ , \quad (9)$$

and hence by (6) we have

$$\tilde{\gamma}_{deg}^{lc}(0) = \tilde{x}_0 \ , \quad \tilde{\gamma}_{deg}^{lc}(s_1) = \tilde{\gamma}_{deg}^{rc}(s_1) = \mathbf{0} \ , \quad \tilde{\gamma}_{deg}^{rc}(1) = \tilde{x}_2 \ . \quad (10)$$

Therefore combining now (8) with $\tilde{x}_1 = \mathbf{0}$ we obtain

$$\tilde{\gamma}_{deg}^{lc}(s) = c_1^{deg}(s - s_1) + c_2^{deg}(s - s_1)^2 + c_3^{deg}(s - s_1)^3 \ ,$$
$$\tilde{\gamma}_{deg}^{rc}(s) = c_1^{deg}(s - s_1) + c_2^{deg}(s - s_1)^2 + d_3^{deg}(s - s_1)^3 \ , \quad (11)$$

with $c_0^{deg} = d_0^{deg} = \mathbf{0}$. The unknown vectors $c_1^{deg}, c_2^{deg}, c_3^{deg}, d_3^{deg}$ appearing in (11) are uniquely determined by solving the following system of four linear vector

ICCS Camera Ready Version 2023
To cite this paper please use the final published version:
DOI: 10.1007/978-3-031-36024-4_34

equations obtained from and (7) and (10):

$$\begin{aligned}
\tilde{x}_0 &= -c_1^{deg}s_1 + c_2^{deg}s_1^2 - c_3^{deg}s_1^3 \ ,\\
\tilde{x}_2 &= c_1^{deg}(1-s_1) + c_2^{deg}(1-s_1)^2 + d_3^{deg}(1-s_1)^3 \ ,\\
\tilde{a}_0 &= 2c_2^{deg} - 6c_3^{deg}s_1 \ ,\\
\tilde{a}_2 &= 2c_2^{deg} + 6d_3^{deg}(1-s_1) \ . \qquad (12)
\end{aligned}$$

An inspection reveals that vector coefficients:

$$\begin{aligned}
c_1^{deg} &= -\frac{\tilde{a}_0s_1^2 - \tilde{a}_2s_1^2 - 2\tilde{a}_0s_1^3 + 2\tilde{a}_2s_1^3 + \tilde{a}_0s_1^4 - \tilde{a}_2s_1^4 - 6\tilde{x}_0 + 12s_1\tilde{x}_0 - 6s_1^2\tilde{x}_0}{6(s_1-1)s_1}\\
&\quad -\frac{6s_1^2\tilde{x}_2}{6(s_1-1)s_1} \ ,\\
c_2^{deg} &= -\frac{-\tilde{a}_2s_1 - \tilde{a}_0s_1^2 + 2\tilde{a}_2\ s_1^2 + \tilde{a}_0s_1^3 - \tilde{a}_2s_1^3 + 6\tilde{x}_0 - 6s_1\tilde{x}_0 + 6s_1\tilde{x}_2}{4(s_1-1)s_1} \ ,\\
c_3^{deg} &= -\frac{-2\tilde{a}_0s_1 - \tilde{a}_2s_1 + \tilde{a}_0s_1^2 + 2\tilde{a}_2s_1^2 + \tilde{a}_0s_1^3 - \tilde{a}_2s_1^3 + 6\tilde{x}_0 - 6s_1\tilde{x}_0 + 6s_1\tilde{x}_2}{12(s_1-1)s_1^2} \ ,\\
d_3^{deg} &= -\frac{-3\tilde{a}_2s_1 - \tilde{a}_0s_1^2 + 4\tilde{a}_2s_1^2 + \tilde{a}_0s_1^3 - \tilde{a}_2s_1^3 + 6\tilde{x}_0 - 6s_1\tilde{x}_0 + 6s_1\tilde{x}_2}{12(s_1-1)^2s_1} \ . \qquad (13)
\end{aligned}$$

solve (as functions in s_1) the system (12). Alternatively one may e.g. use *Mathematica* function *Solve* to find explicit formulas for (13) solving (12). In our special degenerate case of $n=2$ we have $a_0 = a_2 = \mathbf{0}$ (with $\tilde{a}_0 = \tilde{a}_2 = \mathbf{0}$ - see (4)) and thus (13) reads as:

$$\begin{aligned}
c_1^{deg_0} &= -\frac{-6\tilde{x}_0 + 12s_1\tilde{x}_0 - 6s_1^2\tilde{x}_0 + 6s_1^2\tilde{x}_2}{6(s_1-1)s_1} \ ,\\
c_2^{deg_0} &= -\frac{6\tilde{x}_0 - 6s_1\tilde{x}_0 + 6s_1\tilde{x}_2}{4(s_1-1)s_1} \ ,\\
c_3^{deg_0} &= -\frac{6\tilde{x}_0 - 6s_1\tilde{x}_0 + 6s_1\tilde{x}_2}{12(s_1-1)s_1^2} \ ,\\
d_3^{deg_0} &= -\frac{6\tilde{x}_0 - 6s_1\tilde{x}_0 + 6s_1\tilde{x}_2}{12(s_1-1)^2s_1} \ . \qquad (14)
\end{aligned}$$

Note that the formula for the energy $\tilde{\mathcal{E}}_{deg}$ reads as:

$$\tilde{\mathcal{E}}_{deg}(s_1) = \int_0^{s_1} \|\tilde{\gamma}_{deg}^{lc''}(s)\|^2 ds + \int_{s_1}^1 \|\tilde{\gamma}_{deg}^{rc''}(s)\|^2 ds \ . \qquad (15)$$

ICCS Camera Ready Version 2023
To cite this paper please use the final published version:
DOI: 10.1007/978-3-031-36024-4_34

Combining (15) with (11) and (14) yields (upon e.g. using *Mathematica* functions *Integrate* and *FullSimplify*):

$$\tilde{\mathcal{E}}_{deg}(s_1) = \frac{3(\|\tilde{x}_0\|^2(s_1-1)^2 + s_1(\|\tilde{x}_2\|^2 s_1 + (2-2s_1)\langle\tilde{x}_0|\tilde{x}_2\rangle))}{(s_1-1)^2 s_1^2} = 3\left\|\frac{\tilde{x}_0(s_1-1)-\tilde{x}_2 s_1}{(s_1-1)s_1}\right\|^2 , \tag{16}$$

for arbitrary m. To justify the latter one proves first that (16) holds for $m = 1$. Then the same vector version is derived by using m times one dimensional formula with the observation that one dimensional sections of homogeneous boundary conditions $a_0 = a_2 = \mathbf{0}$ are additive. Coupling $\tilde{x}_0 = x_0 - x_1$ and $\tilde{x}_2 = x_2 - x_1$ with (16) yields:

$$\tilde{\mathcal{E}}_{deg}(s_1) = 3\left\|\frac{x_1 - x_0 - s_1(x_2 - x_0)}{(s_1-1)s_1}\right\|^2 . \tag{17}$$

By (16) or (17) we have

$$\lim_{s_1\to 0^+} \tilde{\mathcal{E}}_{deg}(s_1) = \lim_{s_1\to 1^-} \tilde{\mathcal{E}}_{deg}(s_1) = +\infty . \tag{18}$$

Thus as $\tilde{\mathcal{E}}_{deg} \geq 0$, $\tilde{\mathcal{E}}_{deg} \in C^1((0,1))$ there exists a global minimum $s_1^{opt} \in (0,1)$ of $\tilde{\mathcal{E}}_{deg}$ for which $\tilde{\mathcal{E}}'_{deg}$ vanishes. We use next the assumption that $x_i \neq x_{i+1}$ (for $i = 0, 1$) as then $\tilde{x}_0 \neq 0$ and $\tilde{x}_2 \neq 0$. Similarly, (18) holds for $x_0 = x_2$.

An easy inspection shows that (use alternatively symbolic differentiation in *Mathematica* and *FullSimplify*):

$$\tilde{\mathcal{E}}'_{deg}(s_1) = -\frac{6(\|\tilde{x}_0\|^2(s_1-1)^3 + \|\tilde{x}_2\|^2 s_1^3 - (s_1-1)s_1(2s_1-1)\langle\tilde{x}_0|\tilde{x}_2\rangle)}{(s_1-1)^3 s_1^3} . \tag{19}$$

The numerator of (19) is a polynomial of degree 3 ($\tilde{\mathcal{E}}'_{deg}(s_1) = \frac{-1}{(s_1-1)^3 s_1^3} N_{deg}(s_1)$)

$$N_{deg}(s_1) = b_0^{deg} + b_1^{deg} s_1 + b_2^{deg} s_1^2 + b_3^{deg} s_1^3 \tag{20}$$

with vector coefficients $b_j^{deg} \in \mathbb{R}^m$ (for $j = 0, 1, 2, 3$) equal to (apply e.g. *Mathematica* functions *Factor* and *FullSimplify*):

$$\begin{aligned}
\frac{b_0^{deg}}{6} &= -\|\tilde{x}_0\|^2 = -\|x_1\|^2 - \|x_0\|^2 + 2\langle x_0|x_1\rangle , \\
\frac{b_1^{deg}}{6} &= 3\|\tilde{x}_0\|^2 - \langle\tilde{x}_0|\tilde{x}_2\rangle = 3\|x_0\|^2 + 2\|x_1\|^2 - 5\langle x_0|x_1\rangle + \langle x_1|x_2\rangle - \langle x_0|x_2\rangle , \\
\frac{b_2^{deg}}{6} &= 3(\langle\tilde{x}_0|\tilde{x}_2\rangle - \|\tilde{x}_0\|^2) = 3(-\langle x_1|x_2\rangle + \langle x_1|x_0\rangle + \langle x_0|x_2\rangle - \|x_0\|^2) , \\
\frac{b_3^{deg}}{6} &= \|\tilde{x}_2 - \tilde{x}_0\|^2 = \|x_2\|^2 + \|x_0\|^2 - 2\langle x_0|x_2\rangle .
\end{aligned} \tag{21}$$

ICCS Camera Ready Version 2023
To cite this paper please use the final published version:
DOI: 10.1007/978-3-031-36024-4_34

Note that by (16) the sufficient condition for $\mathcal{E}_{deg}$ to vanish is the *colinearity* of shifted data $x_1 - x_0$ and $x_2 - x_1$ and the existence of $s_1^{opt} \in (0,1)$ satisfying $x_1 - x_0 = s_1^{opt}(x_2 - x_0)$. Such s_1^{opt} yields the global minimum of $\mathcal{E}_{deg}$.

In a search for critical points and a global optimum of $\tilde{\mathcal{E}}_{deg}$, one can invoke *Mathematica Package Solve* which can find all roots (real and complex) for a given low order polynomial. Upon computing the roots of (20) we select only these which are real and belong to $(0,1)$. Next we evaluate $\tilde{\mathcal{E}}_{deg}$ on each critical point $s_1^{crit} \in (0,1)$ and choose s_1^{crit} with minimal energy $\tilde{\mathcal{E}}_{deg}$ as global optimizer over $(0,1)$. We shall perform more exhaustive analysis for the existence of critical points of $\tilde{\mathcal{E}}_{deg}$ over $(0,1)$ in Section 3 (for arbitrary m).

3 Critical Points for Degenerate Case

We investigate now the character of critical points for $\tilde{\mathcal{E}}_{deg}$ over the interval $(0,1)$ (for degenerate case of reduced data $\mathcal{M}_n$ with $n=2$). In Section 2 the existence of a global minimum for $\tilde{\mathcal{E}}_{deg}$ over $(0,1)$ is justified.

Example 1. Consider first a special case i.e. of *co-linear data* $\mathcal{M}_n$ for which $\tilde{x}_0 = k\tilde{x}_2$. Recall that cumulative chord assigns to to $\mathcal{M}_n$ the knots $\hat{t}_0 = 0$, $\hat{t}_1 = \|x_1 - x_0\| = \|\tilde{x}_0\|$ and $\hat{t}_2 = \hat{t}_1 + \|x_2 - x_1\| = \|\tilde{x}_0\| + \|\tilde{x}_2\|$. Thus the normalized cumulative chord reads as $s_0^{cc} = 0$, $s_1^{cc} = \|\tilde{x}_0\|/(\|\tilde{x}_0\| + \|\tilde{x}_2\|)$ and $s_2^{cc} = 1$.

For $k < 0$ i.e. *co-linearly ordered data* the cumulative chord $\hat{s}_1^{cc}$ is the global optimizer s_g nullifying $\tilde{\mathcal{E}}_{deg}(s_1^{cc}) = 0$. Indeed by (16) we see that $\tilde{\mathcal{E}}_{deg}$ vanishes if and only if $\tilde{x}_0(1-s_1)+s_1\tilde{x}_2 = \mathbf{0}$. Since $\tilde{x}_0 = k\tilde{x}_2$ we have $(k(1-s_1)+s_1)\tilde{x}_2 = \mathbf{0}$, which as $\tilde{x}_2 \neq \mathbf{0}$ yields $k(1-s_1)+s_1 = 0$ and therefore as $k < 0$ the global optimizer $s_1 = -k/(1-k) = |k|/(1+|k|) \in (0,1)$. The latter coincides with cumulative chord $\hat{s}_1^{cc}$ for $\mathcal{M}_n$. This fact can be independently inferred by defining $x(s) = \tilde{x}_0(1-s) + \tilde{x}_2 s$ which satisfies $x(0) = \tilde{x}_0$, $x(1) = \tilde{x}_2$, $x''(0) = x''(1) = \mathbf{0}$. As $\tilde{x}_0 = k\tilde{x}_2$ with $k < 0$ we also have $x(\hat{s}_1^{cc}) = \tilde{x}_1 = \mathbf{0}$, where $\hat{s}_1^{cc} = |k|/(1+|k|)$ is a cumulative chord. As also $x(s)$ is a piecewise cubic and is of class C^2 at $\hat{s}_1^{cc}$ since $x''(s) \equiv \mathbf{0}$ the curve $x(s)$ minimizes $\tilde{\mathcal{E}}_{deg}$ with $\hat{s}_1^{cc}$.

The case of $k = 0$ in $\tilde{x}_0 = k\tilde{x}_2$ is impossible as otherwise $\tilde{x}_0 = \mathbf{0}$ which leads to $x_0 = x_1$ contradictory to $x_i \neq x_{i+1}$ (for $i = 1,2$).

For $0 < k < 1$ (*co-linearly unordered data*) in $\tilde{x}_0 = k\tilde{x}_2$ the energy at global minimum $\tilde{\mathcal{E}}_{deg}(s_g) > 0$, as otherwise $s_g = k/(k-1) < 0$.

Similarly for $k > 1$ in $\tilde{x}_0 = k\tilde{x}_2$ the energy at global minimum $\tilde{\mathcal{E}}_{deg}(s_g) > 0$ as otherwise $s_g = k/(k-1) > 1$.

Lastly, for $k = 1$ in $\tilde{x}_0 = k\tilde{x}_2$ the energy $\tilde{\mathcal{E}}_{deg}(s_g) > 0$ satisfies $s_g = s_1^{cc} = 1/2$. Indeed, by (16) here $\tilde{\mathcal{E}}_{deg}(s_1) = \|x_0\|^2/((s_1-1)^2 s_1^2) > 0$ (as $x_0 \neq x_1$) and yields a single critical point $s_g = 1/2$ which coincides with $s_1^{cc} = 1/2$ as $\|\tilde{x}_0\| = \|x_2\|$. □

In a search for *all critical points* of $\tilde{\mathcal{E}}_{deg}$ recall (20) and (21) which yield (modulo factor 1/6) $N_{deg}(0) = -\|\tilde{x}_0\|^2 < 0$ and $N_{deg}(1) = \|\tilde{x}_2\|^2 > 0$ - note that the remaining factor in $\tilde{\mathcal{E}}'_{deg}$ is always positive for $s_1 \in (0,1)$ (see (19)). To

ICCS Camera Ready Version 2023
To cite this paper please use the final published version:
DOI: 10.1007/978-3-031-36024-4_34

guarantee the existence of a single critical point it suffices by Intermediate Value Theorem to show that either

$$N'_{deg}(s_1) = c_0^{deg} + c_1^{deg} s_1 + c_2^{deg} s_1^2 > 0$$

over $(0, 1)$ (yielding N_{deg} as strictly increasing with exactly one root $\hat{s}_1 \in (0, 1)$) or that $N'_{deg} = 0$ has exactly one root $\hat{u}_1 \in (0, 1)$ (i.e. N_{deg} has exactly one max/min/saddle at some $\hat{s}_1$). The latter combined with $N_{deg}(0) \cdot N_{deg}(1) < 0$ results in $N_{deg}(s_1) = 0$ having exactly root $\hat{s}_1 \in (0, 1)$ (a critical point of $\tilde{\mathcal{E}}_{deg}$). Note that if $\hat{s}_1 = \hat{u}_1$ then $\hat{u}_1$ is a saddle point of N_{deg}. Here the quadratic $N'_{deg}(s_1)$ has the following coefficients (see (21)):

$$c_0^{deg} = 3\|\tilde{x}_0\|^2 - \langle \tilde{x}_0 | \tilde{x}_2 \rangle \;, c_1^{deg} = 6(\langle \tilde{x}_0 | \tilde{x}_2 \rangle - \|\tilde{x}_0\|^2) \;, c_2^{deg} = 3\|\tilde{x}_2 - \tilde{x}_0\|^2 > 0 \;. \tag{22}$$

We introduce *two auxiliary parameters* $(\lambda, \mu) \in \Omega = (\mathbb{R}_+ \times [-1, 1]) \setminus \{(1, 1)\}$:

$$\|\tilde{x}_0\| = \lambda \|\tilde{x}_2\| \;, \quad \langle \tilde{x}_0 | \tilde{x}_2 \rangle = \mu \|\tilde{x}_0\| \|\tilde{x}_2\| \;. \tag{23}$$

Note that geometrically μ stands for $\cos(\alpha)$, where α is the angle between vectors $\tilde{x}_0$ and $\tilde{x}_2$ - hence $\mu = \lambda = 1$ results in $\tilde{x}_0 = \tilde{x}_2$. Such case is analyzed in Ex. 1 for $k = 1$ rendering $(\mu, \lambda) = (1, 1)$ as admissible.

Upon substituting two parameters $(\mu, \lambda) \in \Omega$ (see (23)) into $N'_{deg}(s_1) > 0$ (see also (22)) we arrive at genuine quadratic inequality in $u \in (0, 1)$ (for $u = s_1$):

$$W_{\lambda\mu}(u) = 3\lambda^2 - \mu\lambda + u(6\mu\lambda - 6\lambda^2) + u^2(3\lambda^2 - 6\mu\lambda + 3) > 0 \;, \tag{24}$$

with positive coefficient (standing with u^2) as $3\lambda^2 - 6\mu\lambda + 3 = 3((\lambda - \mu)^2 + 1 - \mu^2) > 0$ over Ω.

We examine now various constraints on $(\mu, \lambda) \in \Omega$ ensuring existence of either no roots of the quadratic $N'_{deg}(s_1) = 0$ (as then since $N_{deg}(0) < 0$ and $N_{deg}(1) > 0$ a cubic N_{deg} is an increasing function) or exactly one root of the quadratic $N'_{deg}(s_1) = 0$ over $(0, 1)$. As already pointed out the satisfaction of both these cases yield exactly one critical point of $\tilde{\mathcal{E}}_{deg}$). The discriminant $\tilde{\Delta}_{crit}$ for $W_{\lambda\mu}(u) = 0$ (see (24)) reads as:

$$\tilde{\Delta}_{deg}(\mu, \lambda) = 12\lambda(-3\lambda + \mu + \lambda^2\mu + \lambda\mu^2) \;.$$

We consider now 3 cases in a search for admissible zones to enforce unimodality of $\tilde{\mathcal{E}}_{deg}$.

1. $\tilde{\Delta} < 0$. Here N'_{deg} has no real roots over $(0, 1)$. Since $c_2^{deg} > 0$, clearly $N'_{deg} > 0$ over $(0, 1)$ - note here $N_{deg}(0) < 0$ and $N_{deg}(1) > 0$. The latter inequality amounts to (with $\Delta_{deg} = (\tilde{\Delta}_{deg}/12\lambda$ and $\lambda > 0$)

$$\Delta_{deg} = -3\lambda + \mu + \lambda^2\mu + \lambda\mu^2 < 0 \;. \tag{25}$$

In order to decompose Ω into subregions Ω_- (with $\Delta_{deg} < 0$), Ω_+ (with $\Delta_{deg} > 0$) and Γ_0 (with $\Delta_{deg} \equiv 0$) we resort to *Mathematica* functions *InequalityPlot*,

ICCS Camera Ready Version 2023
To cite this paper please use the final published version:
DOI: 10.1007/978-3-031-36024-4_34

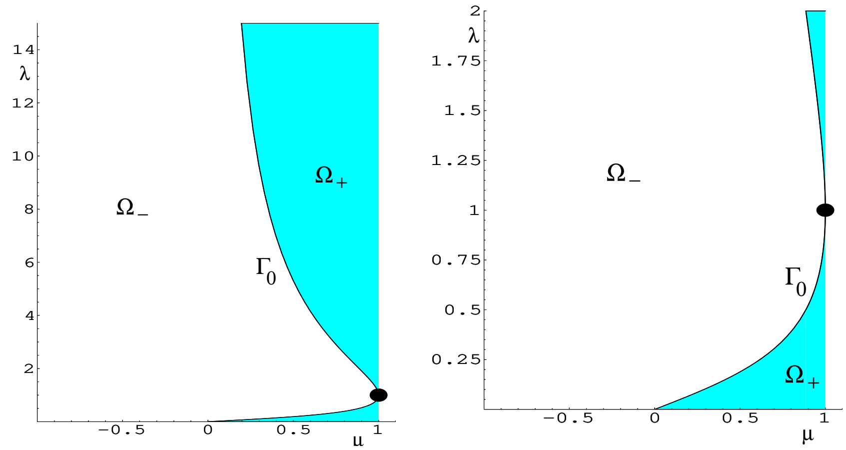

(a) (b)

Fig. 1. Decomposition of Ω into subregions: (a) over which $\Delta_{deg} > 0$ (i.e. Ω_+), $\Delta_{deg} = 0$ (i.e. Γ_0) or $\Delta_{deg} < 0$ (i.e. Ω_-), (b) only for λ small.

ImplicitPlot and *Solve*. Figure 1(a) shows the resulting decomposition and Figure 1(b) shows its magnification for λ small. The intersection points of Γ_0 and boundary $\partial\Omega$ (found by *Solve*) read: for $\mu = 1$ it is a point $(1, 1)$ (already excluded though analyzed - see dotted point in Figure 1), for $\mu = -1$ it is a point $(-1, 0)$ (excluded as $\lambda > 0$) and for $\lambda = 0$ it is a point $(0, 0) \notin \Omega$ (also excluded as $\lambda > 0$).

The admissible subset $\Omega_{ok} \subset \Omega$ of parameters (μ, λ) (for which there is one local minimum of $\tilde{\mathcal{E}}_{deg}$ and thus a unique global one) satisfies $\Omega_- \subset \Omega_{ok}$. The complementary set to $\Omega \setminus \Omega_-$ forms a potential *exclusion zone* i.e. $\Omega_{ex} \subset \Omega \setminus \Omega_-$. Next we limit furthermore an exclusion zone $\Omega_{ex} \subset \Omega$ (currently not bigger than shaded region in Figure 1).

2. $\tilde{\Delta}_{deg} = 0$. There is only one root $\hat{u}_1^0 \in \mathbb{R}$ of $N'_{deg}(s_1) = 0$. As already explained, irrespectively whether $\hat{u}_1^0 \in (0, 1)$ or $\hat{u}_1^0 \notin (0, 1)$ this results in exactly one root $\hat{s}_1 \in (0, 1)$ of $N_{deg}(s_1) = 0$, which in turn yields exactly one local minimum for $\tilde{\mathcal{E}}_{deg}$ (turning out to be a global one). Hence $\Omega_- \cup \Gamma_0 \subset \Omega_{ok}$.

3. $\tilde{\Delta}_{deg} > 0$. There are two different roots $\hat{u}_1^{\pm} \in \mathbb{R}$ of $N'_{deg}(s_1) = 0$. They are either (in all cases we use Vieta's formulas):

(a) of *opposite signs*: i.e. $(c_0^{deg}/c_2^{deg}) < 0$ or

(b) non-positive: i.e. $(c_0^{deg}/c_2^{deg}) \geq 0$ and $(-c_1^{deg}/c_2^{deg}) < 0$ (here $\hat{u}_1^- < \hat{u}_1^+$ as $c_2^{deg} > 0$) or

(c) non-negative: i.e. $(c_0^{deg}/c_2^{deg}) \geq 0$ and $(-c_1^{deg}/c_2^{deg}) > 0$ - split into:

(c1) $\hat{u}_1^+ \geq 1$: i.e.

(c2) $0 < \hat{u}_1^+ < 1$ (recall $\hat{u}_1^- < \hat{u}_1^+$).

ICCS Camera Ready Version 2023
To cite this paper please use the final published version:
DOI: 10.1007/978-3-031-36024-4_34

Evidently cases *a)*, *b)* and *c1)* yield *up to one root* $\hat{u}_1 \in (0,1)$ of $N_i^{deg'}(s_1) = 0$. Hence as already explained there is only one root $\hat{s}_1 \in (0,1)$ of $N_i^{deg}(s_1) = 0$, which is the unique critical point of $\tilde{\mathcal{E}}^c_{deg}$ over $(0,1)$ (in fact a global minimum).

In the next step we show that *the inequalities* from *a)* or *b)* or *c1)* *extend (contract) the admissible (exclusion) zone* to $\Omega_{ok} = \Omega$ (to $\Omega_{ex} = \emptyset$). Indeed:

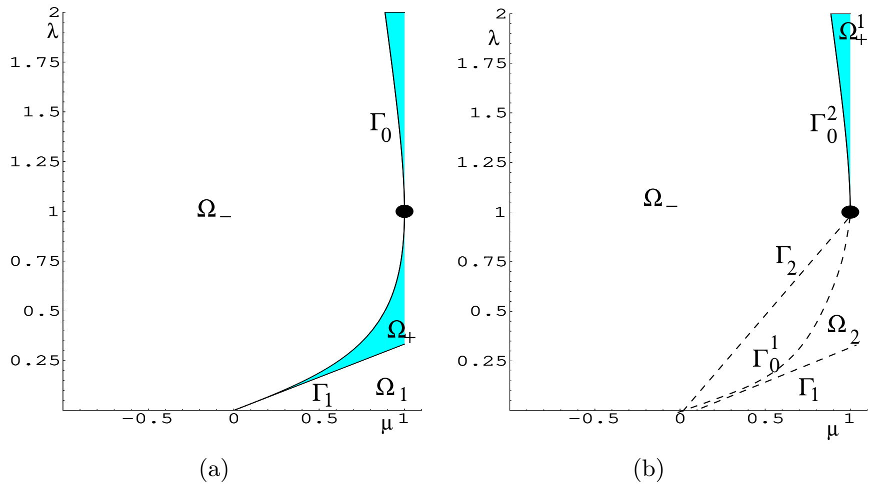

Fig. 2. Extension of admissible zone Ω_{ok} by cutting from exclusion zone Ω_{ex}: (a) Ω_1, (b) Ω_2.

a) the constraint $(c_0^{deg}/c_2^{deg}) < 0$ upon using (24) reads (as $\lambda > 0$ and $c_2^{deg} > 0$):

$$3\lambda^2 - \mu\lambda < 0 \quad \equiv \lambda < \frac{\mu}{3}\,. \tag{26}$$

Figure 2 a) shows Ω_1 (over which (26) holds) cut out from the exclusion zone Ω_{ex} of parameters $(\mu,\lambda) \in \Omega$ (again *Mathematica InequalityPlot* is used here). Thus $\Omega_- \cup \Gamma_0 \cup \Omega_1 \subset \Omega_{ok}$. The intersection $\Gamma_1 \cap \partial\Omega = \{(0,0),(1,1/3)\}$ (here $\Gamma_1 = \{(\mu,\lambda) \in \Omega : 3\lambda - \mu = 0\}$) and $\Gamma_0 \cap \Gamma_1 = \{(0,0)\}$ (we invoke here *Solve* function).

b) the constraints $(c_0^{deg}/c_2^{deg}) \geq 0$ and $(-c_1^{deg}/c_2^{deg}) < 0$ combined with (24) yield:

$$\lambda \geq \frac{\mu}{3} \quad \text{and} \quad ((6\mu\lambda - 6\lambda^2) > 0 \quad \equiv \lambda < \mu)\,. \tag{27}$$

Again with the aid of *ImplicitPlot* and *InequalityPlot* we find $\Omega_2 \cup \Gamma_1$ (to be cut out of Ω_{ok}) as the intersection of three sets determined by (27) and $\Delta > 0$ (for Ω_2 see Figure 2 b) - a set bounded by Γ_0^1, Γ_1). Thus the admissible set

ICCS Camera Ready Version 2023
To cite this paper please use the final published version:
DOI: 10.1007/978-3-031-36024-4_34

Ω_{ok} satisfies $\Omega_- \cup \Gamma_0 \cup \Omega_1 \cup \Omega_2 \cup \Gamma_1 \subset \Omega_{ok}$ (see Figure 2 b)). Note that for $\Gamma_2 = \{(\mu, \lambda) \in \Omega : \mu - \lambda = 0\}$ the intersection of curves $\Gamma_0 \cap \Gamma_2 = \{(0,0),(1,1)\}$ and $\Gamma_1 \cap \Gamma_2 = \{(0,0)\}$, and of Γ_2 with the boundary $\partial\Omega$ $\{(0,0),(1,1)\}\}$ (use e.g. *Solve*). The exclusion zone Ω_{ex} must now satisfy $\Omega_{ex} \subset \Omega_+^1$ (see Figure 2 b)).

c1) the constraints $(c_0^{deg}/c_2^{deg}) \geq 0$, $(-c_1^{deg}/c_2^{deg}) > 0$ and $u_1^+ \geq 1$ combined with (24) render (as $c_2^{deg} > 0$):

$$\lambda \geq \frac{\mu}{3}\,, \quad \lambda > \mu\,, \quad \sqrt{\tilde{\Delta}_{deg}} \geq 6(1-\lambda\mu)\,. \tag{28}$$

As we are only interested in reducing Ω_+^1 one intersects first the corresponding two sets (determined by the first two inequalities in (28)) with Ω_+^1 which clearly yields Ω_+^1. To complete solving (28) it suffices to find the intersection of Ω_+^1 with the set determined by the third inequality of (28). Note that for $(\mu, \lambda) \in \Omega_+^1$ we have $\mu > 0$. Indeed, by inspection or by applying the *Mathematica* function *Solve* to $\tilde{\Delta}_{deg}(\mu, \lambda) = 0$ (with $\mu(\lambda)$ treated as variable and λ as parameter) by (25) we have

$$\mu_\pm(\lambda) = \frac{-1 - \lambda^2 \pm \sqrt{1 + 14\lambda^2 + \lambda^4}}{2\lambda}\,.$$

A simple verification shows that $\mu_+ > 0$ as $12\lambda^2 > 0$ (since $\lambda > 0$ over Ω_+^1). Similarly $\mu_- < -1$ as $-\sqrt{1 + 14\lambda^2 + \lambda^4} < (1-\lambda)^2$ holds. Thus for a fixed pair $(\mu, \lambda) \in \Omega_+^1$ (where $\tilde{\Delta}_{deg}(\mu, \lambda) > 0$) we must have $\mu(\lambda) \in (-\infty, \mu_-) \cup (\mu_+, +\infty)$. The latter intersected with $\mu \in [-1, 1]$ yields that $0 < \mu$ for all pairs $(\mu, \lambda) \in \Omega_+^1$. We show now that the third inequality in (28) results in $\Omega_{ex} = \emptyset$. Indeed note that $\sqrt{\tilde{\Delta}_{deg}} \geq 6(1-\lambda\mu)$ is satisfied if $1 - \lambda\mu < 0$ which is equivalent (as $\mu > 0$ - shown to hold over Ω_+^1) to $\lambda > 1/\mu$ (for $\mu \in (0,1]$). The case when $1 - \lambda\mu \geq 0$ yields $\lambda \leq 1/\mu$ which gives the set not intersecting with Ω_+^1. *Mathematica* function *InequalityPlot* yields the region $\Omega_5 = \Omega_3 \cup \Omega_4 \cap \Gamma_0^2$ (bounded by the curve $\Gamma_3 = \{(\mu, \lambda) \in \Omega : 1 - \mu\lambda = 0,\ \mu > 0\}$ and the boundary $\partial\Omega$ - see Figure 3). Clearly as $\Omega_4 = \Omega_+^1$ we can cut out from Ω_{ex} the set Ω_+^1 and thus $\Omega_{ex} = \emptyset$ (or $\Omega_{ok} = \Omega$). Hence there is only one critical point of $\tilde{\mathcal{E}}_0^{deg}$ over $(0,1)$.

The last geometric argument exploits the observation that Γ_0^2 is positioned above Γ_3. To show the latter algebraically one solves $\tilde{\Delta}_{deg} = 0$ in $\lambda(\mu)$ (use e.g. *NSolve*) by treating λ as variable and μ as a parameter. We obtain then (see (25))

$$\lambda_\pm(\mu) = \frac{3 - \mu^2 \pm \sqrt{9 - 10\mu^2 + \mu^4}}{2\mu}\,.$$

Note that the expression inside the square root is always non-negative. It suffices to show now that $\lambda_\pm(\mu) > \lambda_1(\mu) = 1/\mu$ for all $(\mu, \lambda) \in (0,1] \times (1, +\infty)$. The inequality $\lambda_+(\mu) > \lambda_1(\mu)$ holds as for $\mu > 0$ it amounts to

$$\sqrt{9 - 10\mu^2 + \mu^4} > \mu^2 - 1\,.$$

ICCS Camera Ready Version 2023
To cite this paper please use the final published version:
DOI: 10.1007/978-3-031-36024-4_34

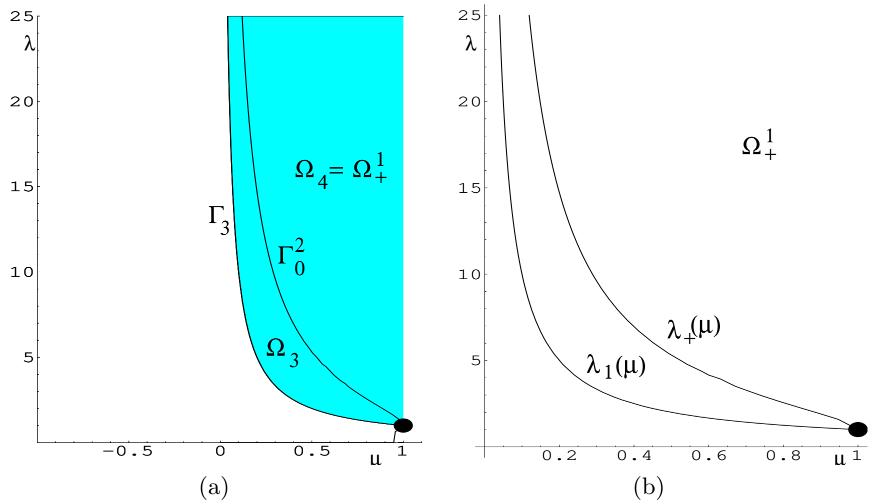

Fig. 3. (a) Cutting from Ω_{ex} the set $\Omega_5 = \Omega_3 \cup \Omega_4 \cup \Gamma_0^2$, (b) The graphs of two functions $\lambda_1(\mu)$ and $\lambda_+(\mu)$.

The latter holds as $\mu^2 - 1 < 0$ for $\mu \neq \pm 1$ - $\mu = -1$ excluded and $\mu = 1$ results in $\lambda_+(1) = 1$ which also is excluded as $(1,1) \notin \Omega$. The second function $\lambda_-(\mu)$ cannot be bigger that $\lambda_1(\mu)$ and thus is excluded. Indeed for $\mu \in [0,1)$ the latter would amount to

$$-\sqrt{9 - 10\mu^2 + \mu^4} \geq \mu^2 - 1 \,.$$

As both sides are non-positive we have

$$(9 - 10\mu^2 + \mu^4) \leq (\mu^2 - 1)^2$$

which is false as $8(1 - \mu^2) \leq 0$ does not hold for $\mu \in [0,1)$. Recall that $\mu = 1$ would result here in $\lambda_-(\mu) = 1$, which gives already excluded pair $(1,1)$.

Thus for the degenerate case we proved that there is always *exactly one critical point* of $\tilde{\mathcal{E}}_{deg}$ over $(0,1)$. However if we wish to have global minimum of $\tilde{\mathcal{E}}_{deg}$ to be close to cumulative chord $\hat{s}_1^{cc}$ (which optimizes special case of co-linear data) then the perturbation analysis (similar to the generic and non-generic case of Leap-Frog algorithm - see [6, 7]) can be invoked. Note also if Decartes's sign rule is applied to $N_{deg}(s_1) = 0$ (see (20)) since $b_0^{deg} > 0$ and $b_3^{deg} < 0$ a sufficient condtion for one positive rule is that $b_1^{deg} b_2^{deg} \geq 0$. A simple verification shows that this condtion does not yield unique critical point of $\tilde{\mathcal{E}}'_{deg}$ for arbitrary data $\{\tilde{x}_0, \tilde{x}_1, \tilde{x}_2\}$.

4 Experiments

We illustrate now the theoretical results from Section 3 in the following example.

ICCS Camera Ready Version 2023
To cite this paper please use the final published version:
DOI: 10.1007/978-3-031-36024-4_34

Example 2. Consider first three ordered co-linear points $\tilde{x}_2 = (-1, -3)$, $\tilde{x}_0 = k\tilde{x}_2 = (3, 9)$ (with $k = -3$) $\tilde{x}_1 = \mathbf{0}$. The cumulative chord $\hat{s}_1^{cc} = |k|/(1 + |k|) = 3/4$ is expected to be the global minimum (also the only critical point) of $\tilde{\mathcal{E}}_{deg}$ at which the energy vanishes. Indeed the corresponding formula for $\tilde{\mathcal{E}}_{deg}$ (see (16)) reads here as:

$$\tilde{\mathcal{E}}_{deg}(s) = \frac{30(4s-3)^2}{(s-1)^2 s^2} .$$

The *Mathematica Plot* function (used here for all tests in this example) renders the graph of $\tilde{\mathcal{E}}_{deg}$ with global minimum attained at $\hat{s} = \hat{s}_1^{cc}$ satisfying $\tilde{\mathcal{E}}_{deg}(\hat{s}_1^{cc}) = 0$ (see Figure 4 a)).

A slight perturbation of the co-linearity conditions with $\tilde{x}_0 = (3, 10)$ and $\tilde{x}_2$ unchanged yields the energy $\tilde{\mathcal{E}}_{deg}$ (see (16))

$$\tilde{\mathcal{E}}_{deg}(s) = \frac{3(109 - 284s + 185s^2)}{(s-1)^2 s^2} .$$

Again *Mathematica Plot* function renders the graph of $\tilde{\mathcal{E}}_{deg}$ with one global minimum at $\hat{s}_1 \approx 0.76748$ (see Figure 4 b) and c)). Cumulative chord, which reads here $\hat{s}_1^{cc} \approx 0.767524$, together with $\hat{s}_1$ satisfy $0.509341 \approx \tilde{\mathcal{E}}_{deg}(\hat{s}_1) < \tilde{\mathcal{E}}_{deg}(\hat{s}_1^{cc}) \approx 0.509375$.

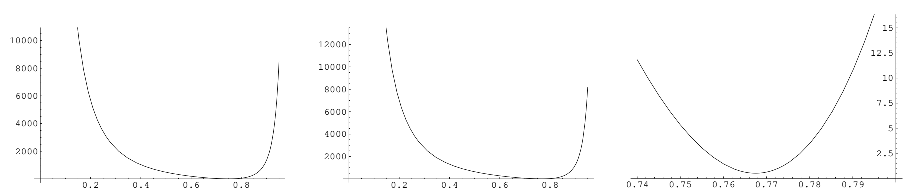

(a) (b) (c)

Fig. 4. The graphs of $\tilde{\mathcal{E}}_{deg}$ for (a) co-linear data $\tilde{x}_0 = (3, 9)$, $\tilde{x}_1 = (0, 0)$ and $\tilde{x}_2 = (-1, -3)$ vanishing at a global minimum $\hat{s}_1^{cc} = 3/4$, (b) slightly non-co-linear data $\tilde{x}_0 = (3, 10)$, $\tilde{x}_1 = (0, 0)$ and $\tilde{x}_2 = (-1, -3)$ non-vanishing at a global minimum at $\hat{s}_1 = 0.76748 \neq \hat{s}_1^{cc} = 0.767524$, (c) as in (b) but with visible $\hat{\mathcal{E}}_{deg}(\hat{s}_1) = 0.509341 > 0$.

On the other hand adding a large perturbation to the co-linearity by taking e.g. $\tilde{x}_0 = (4, -15)$ and $\tilde{x}_2$ unchanged yields the corresponding energy $\tilde{\mathcal{E}}_{deg}$ (see (16))

$$\tilde{\mathcal{E}}_{deg}(s) = \frac{3(241 - 400s + 169s^2)}{(s-1)^2 s^2} .$$

Again *Mathematica Plot* function renders the graph of $\tilde{\mathcal{E}}_{deg}$ with one global minimum at $\hat{s}_1 \approx 0.695985$ (see Figure 5 a) and b)). Cumulative chord which reads

ICCS Camera Ready Version 2023
To cite this paper please use the final published version:
DOI: 10.1007/978-3-031-36024-4_34

here $\hat{s}_1^{cc} \approx 0.830772$, together with $\hat{s}_1$ satisfy $2979.8 \approx \tilde{\mathcal{E}}_{deg}(\hat{s}_1) < \tilde{\mathcal{E}}_{deg}(\hat{s}_1^{cc}) \approx 3844.87$. The value $\tilde{\mathcal{E}}_{deg}(\hat{s}_1) = 2979.8 >> 0$ (see Figure 5 a) and b)).

Finally, for $\tilde{x}_0 = (0.05, -1)$ and $\tilde{x}_2$ unchanged the corresponding energy $\tilde{\mathcal{E}}_{deg}$ (see (16)) reads

$$\tilde{\mathcal{E}}_{deg}(s) = \frac{15.3075(0.196472 + 0.763351s + s^2)}{s^2(s-1)^2} .$$

Again *Mathematica Plot* function renders the graph of $\tilde{\mathcal{E}}_{deg}$ with one global minimum at $\hat{s}_1 \approx 0.357839$ (see Figure 5 c)). Cumulative chord which reads here $\hat{s}_1^{cc} \approx 0.240481$, together with $\hat{s}_1$ satisfy $173.264 \approx \tilde{\mathcal{E}}_{deg}(\hat{s}_1) < \tilde{\mathcal{E}}_{deg}(\hat{s}_1^{cc}) \approx 200.916$. Again, the value $\tilde{\mathcal{E}}_{deg}(\hat{s}_1) = 173.264 > 0$ (see Figure 5 c)). □

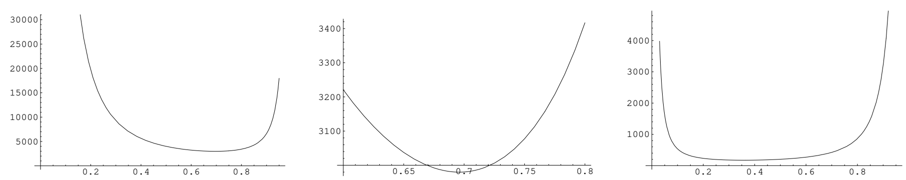

(a) (b) (c)

Fig. 5. The graphs of $\tilde{\mathcal{E}}_{deg}$ for (a) strongly non-co-linear data $\tilde{x}_0 = (4, -15)$, $\tilde{x}_1 = (0, 0)$ and $\tilde{x}_2 = (-1, -3)$ non-vanishing at a global minimum $\hat{s}_1 \approx 0.695985 \neq \hat{s}_1^{cc} \approx 0.830772$, (b) as in (a) but with visible $\tilde{\mathcal{E}}_{deg}(\hat{s}_1) = 2979.8 >> 0$, (c) non-co-linear data $\tilde{x}_0 = (0.05, -1)$, $\tilde{x}_1 = (0, 0)$ and $\tilde{x}_2 = (-1, -3)$ non-vanishing at a global minimum $\hat{s}_1 \approx 0.357839 \neq \hat{s}_1^{cc} \approx 0.240481$, here $\tilde{\mathcal{E}}_{deg}(\hat{s}_1) = 173.264 > 0$.

5 Conclusions

In this work *the unimodality of optimization task* (2) to fit reduced data $\mathcal{M}_n$ is proved for for $n = 2$. The latter constitutes a degenerate variant of (1) investigated earlier for $n \geq 3$ in the context of using Leap-Frog algorithm. This scheme forms an iterative numerical tool to compute the substitutes of the unknown interpolation knots for $n \geq 3$ while minimizing (1) - see [3, 4, 6, 7, 9]. In contrast to the degenerate case of reduced data i.e. to $\mathcal{M}_2$, local iterative univariate functions of Leap-Frog are not in general unimodal though some specific sufficient conditions enforcing the latter are established in [6, 7]. Minimizing the univariate and unimodal function (2) makes any numerical scheme to compute the unique global minimum (i.e. an optimal knot t_1) insensitive to the choice of initial guess which e.g. can be taken e.g. as cumulative chord. More information on Leap-Frog in the context of other applications can be found among all in [14, 15].

ICCS Camera Ready Version 2023
To cite this paper please use the final published version:
DOI: 10.1007/978-3-031-36024-4_34

References

1. de Boor, C.: A Practical Guide to Splines. 2nd edn. Springer-Verlag, New York (2001). https://www.springer.com/gp/book/9780387953663
2. Farouki, R.T.: Optimal parameterizations. Comput. Aided Geom. Des. **14**(2), 153–168 (1997). https://doi.org/10.1016/S0167-8396(96)00026-X
3. Kozera, R., Noakes L.: Optimal knots selection for sparse reduced data. In: Huang, F., Sugimoto, A. (eds.) PSIVT 2015, pp. 3–14. LNCS Vol. 9555, Springer Int. Pub. (2016). https://doi.org/10.1007/978-3-319-30285-0_1
4. Kozera, R., Noakes L.: Non-linearity and non-convexity in optimal knots selection for sparse reduced data. In: Gerdt, V.P., et al. (eds.) CASC 2017, pp. 257–271. LNCS vol. 10490, Springer Int. Pub. (2017). https://doi.org/10.1007/978-3-319-66320-3_19
5. Kozera, R., Noakes L., Wilkołazka, M.: Parameterizations and Lagrange cubics for fitting multidimensional data. In: Krzhizhanovskaya, V.V., et al. (eds.) ICCS 2020, pp. 124–140. LNCS vol. 12138, Springer Cham (2020). https://doi.org/10.1007/978-3-030-50417-5_10
6. Kozera, R., Noakes L., Wiliński, A.: Generic case of Leap-Frog Algorithm for optimal knots selection in fitting reduced data. In: Paszyński, M., et al. (eds.) ICCS 2021, pp. 337–350. LNCS vol. 12745, Part IV, Springer Nature Switzerland AG (2021). https://doi.org/10.1007/978-3-030-77970-2_26
7. Kozera, R., Noakes L.: Non-generic case of Leap-Frog Algorithm for optimal knots selection in fitting reduced data. In: Groen, D., et al. (eds.) ICCS 2022, pp. 341–354. LNCS vol. 13352, Part III, Springer Cham (2022). https://doi.org/10.1007/978-3-031-08757-8_29
8. Kozera, R., Noakes L., Wilkołazka, M.: Exponential parameterization to fit reduced data. Appl. Math. Comput. **391**, 125645 (2021). https://doi.org/10.1016/j.amc.2020.125645
9. Kozera, R., Wiliński A.: Fitting dense and sparse reduced data. In: Pejaś, J. et al. (eds.) ACS 2018, pp. 3–17. In: Advances in Intelligent Systems and Computing vol. 889, Springer Nature Switzerland AG (2019). https://doi.org/10.1007/978-3-030-03314-9_1
10. Kuznetsov, E.B., Yakimovich A.Y.: The best parameterization for parametric interpolation. J. Comput. Appl. Math. **191**(2), 239–245 (2006). https://core.ac.uk/download/pdf/81959885.pdf
11. Kvasov, B.I.: Methods of Shape-Preserving Spline Approximation. World Scientific Pub., Singapore (2000). https://doi.org/10.1142/4172
12. Lee, E.T.Y.: Choosing nodes in parametric curve interpolation. Comput. Aided Des. **21**(6), 363–370 (1989). https://doi.org/10.1016/0010-4485(89)90003-1
13. Matebese, B., Withey, D., Banda M.K.: Modified Newton's method in the Leapfrog method for mobile robot path planning. In: Dash, S.S., et al. (eds.) ICAIECES 2017, pp. 71–78. Advances in Intelligent Systems and Computing vol. 668, Springer Nature Singapore (2018). https://doi.org/10.1007/978-981-10-7868-2_7
14. Noakes, L.: A global algorithm for geodesics. J. Aust. Math. Soc. Series A **65**(1), 37–50 (1998). https://doi.org/10.1017/S1446788700039380
15. Noakes, L., Kozera, R.: Nonlinearities and noise reduction in 3-source photometric stereo. J. Math. Imaging Vision **18**(2), 119–127 (2003). https://doi.org/10.1023/A:1022104332058
16. Piegl, L., Tiller, W.: The NURBS Book. Springer-Verlag, Berlin Heidelberg (1997). https://doi.org/10.1007/978-3-642-97385-7